Supplementary Information

Dynamic formation of nanostructured particles from vesicles via invertase hydrolysis for on-demand delivery

Wye-Khay Fong[a,b*], Antoni Sánchez-Ferrer[a], Francesco Giovanni Ortelli[a], Wenjie Sun[a], Ben J. Boyd[b,c], and Raffaele Mezzenga[a*]

[a]ETH Zürich, Department of Health Sciences & Technology, 8092 Zürich, Switzerland; [b]Drug Delivery, Disposition & Dynamics, Monash Institute of Pharmaceutical Sciences, Monash University, 381 Royal Parade, Parkville, Victoria 3052, Australia. [c]ARC Centre of Excellence in Convergent Bio-Nano Science and Technology, Monash Institute of Pharmaceutical Sciences, Monash University (Parkville Campus), 381 Royal Parade, Parkville, Australia

*Corresponding Authors: raffaele.mezzenga@hest.ethz.ch, khay.fong@monash.edu

Time Resolved SAXS: The effect of invertase on MLO based vesicles

A. MLO+30%SL

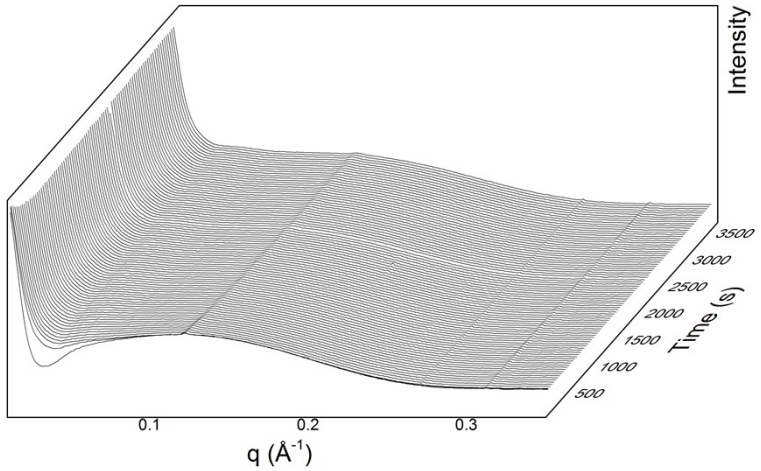

B. MLO+30%SS

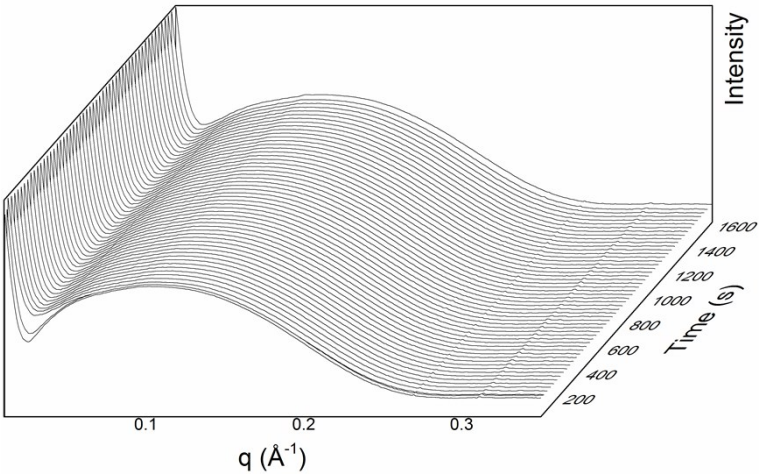

C. MLO

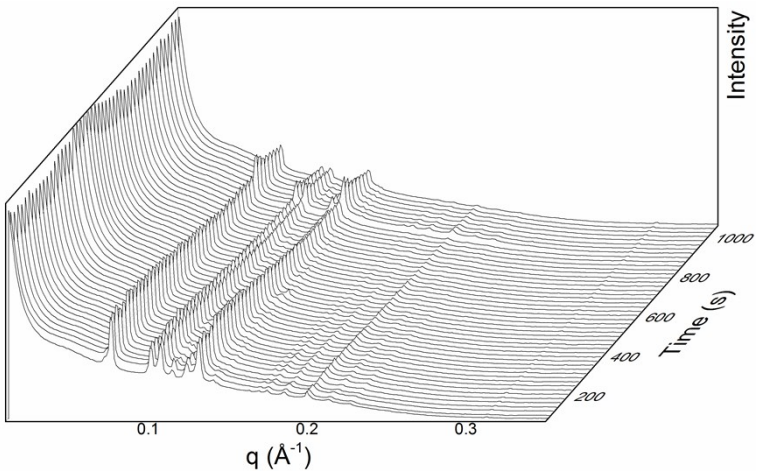

Fig. SI1 – TRSAXS profiles of MLO based dispersions. Invertase digestion of A. vesicles formed by MLO + 30% sucrose laurate B. vesicles formed by MLO + 40% sucrose stearate, and C. MLO cubosomes. No alteration in phase behaviour was observed.

In contrast to the PHYT systems, the MLO based systems were not responsive to invertase digestion as no change in nanostructure or in peak intensity upon addition of invertase was observed (Fig. SI1). Invertase does not appear to affect the phase behaviour of the MLO based vesicles formed by the addition of sucrose esters and MLO cubosomes.

NMR – Quantification of the substitution of the laurate tail onto the sucrose headgroup

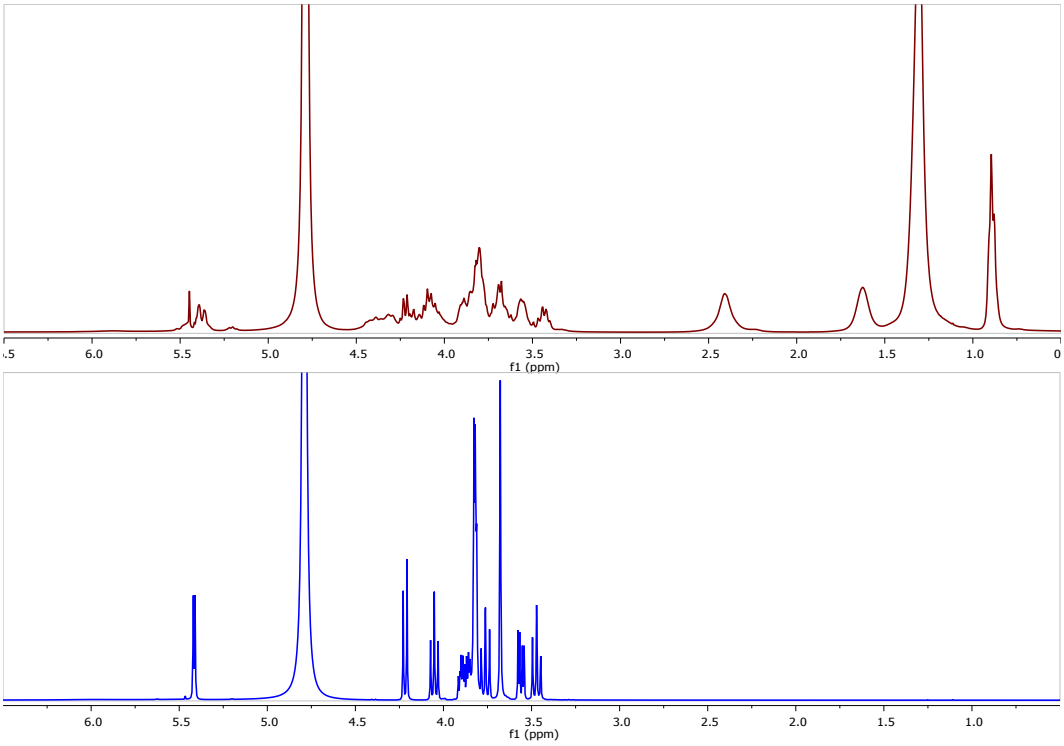

Figure SI2a – ^{1}H NMR spectrum of sucrose laurate in D_2O (red) and sucrose in D_2O (blue)

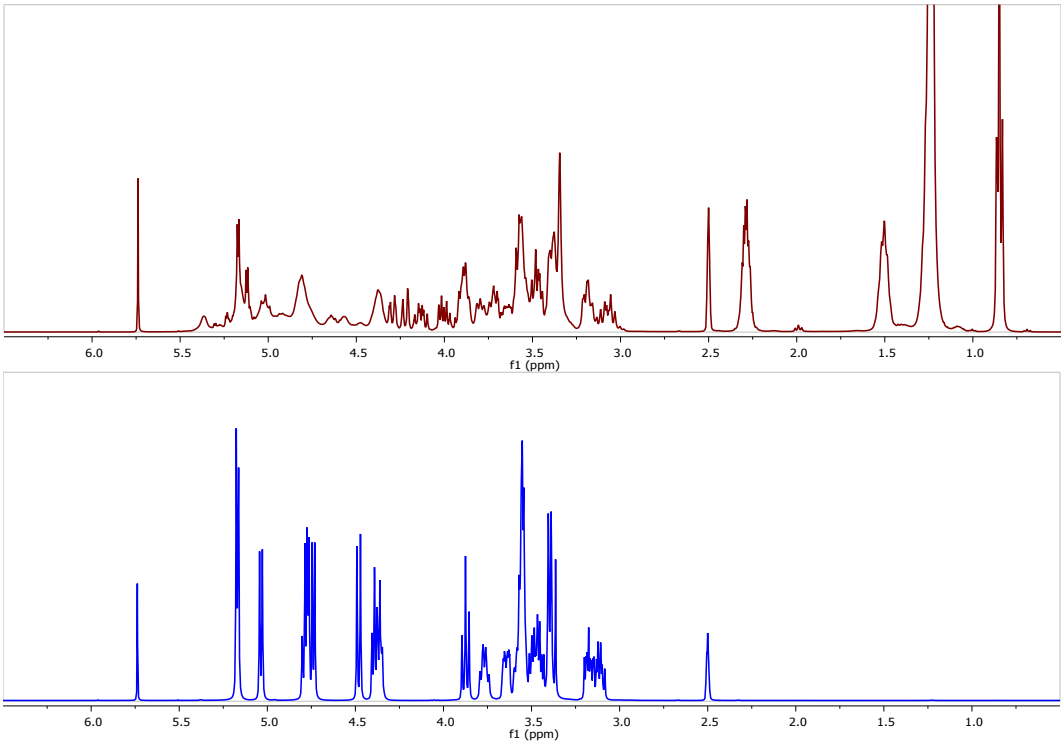

Figure SI2b – ^{1}H NMR spectrum of sucrose laurate in DMSO-d_6 (red) and sucrose in DMSO-d_6 (blue)

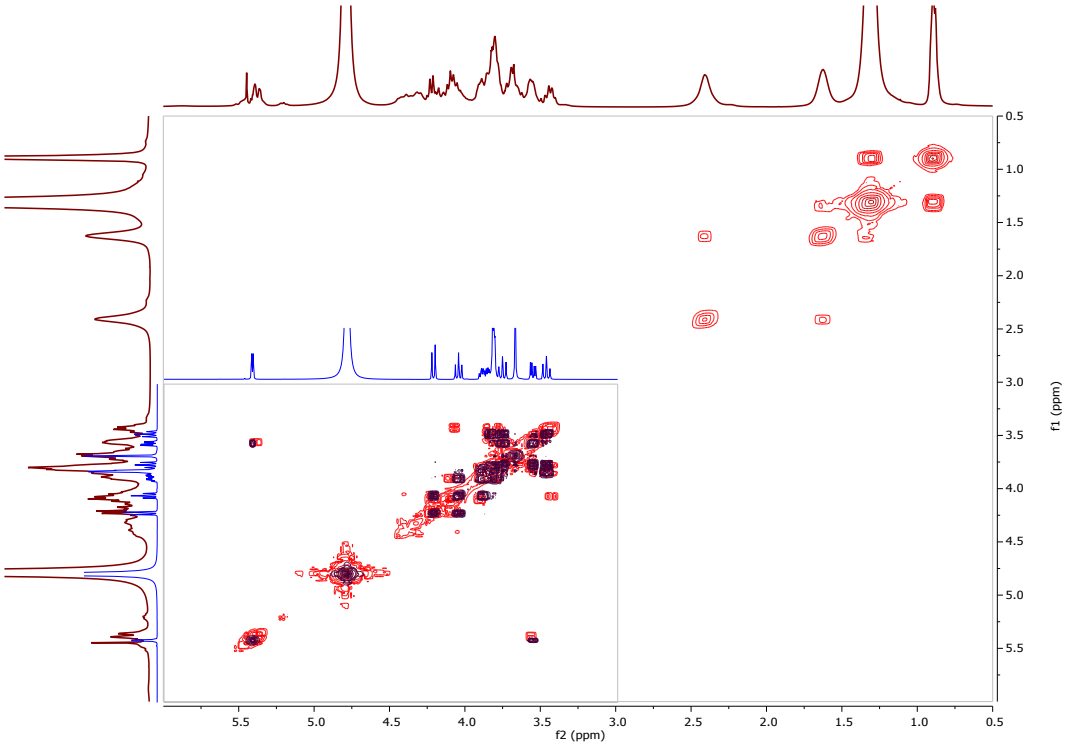

Figure SI2c – ^{1}H-^{1}H NMR spectrum (COSY) of sucrose laurate in D_2O (red) and sucrose in D_2O (blue)

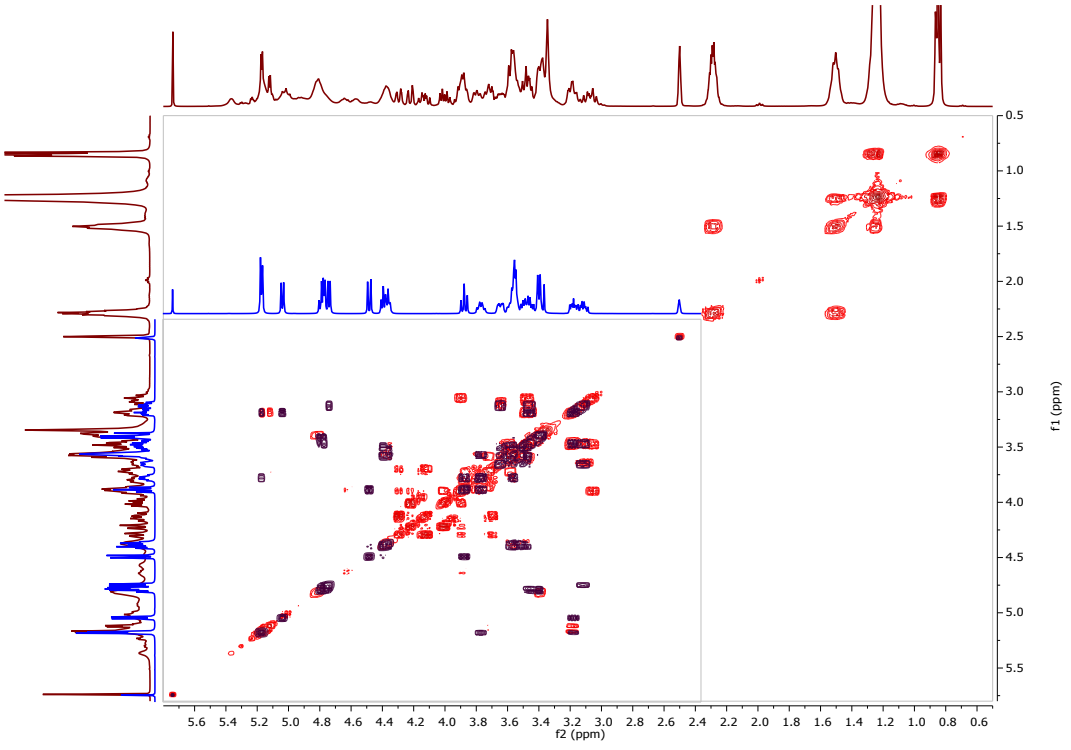

Figure SI2d – ^{1}H-^{1}H NMR (COSY) spectrum of sucrose laurate in DMSO-d_6 (red) and sucrose in DMSO-d_6 (blue)

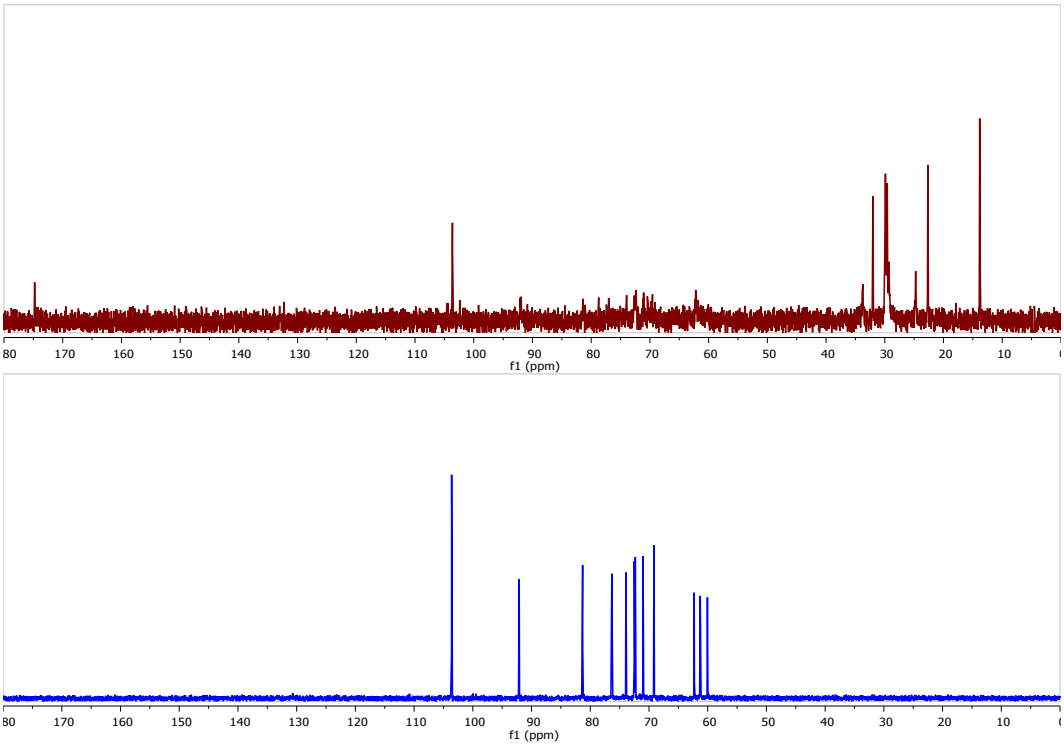

Figure SI2e – ^{13}C NMR spectrum of sucrose laurate in D_2O (red) and sucrose in D_2O (blue)

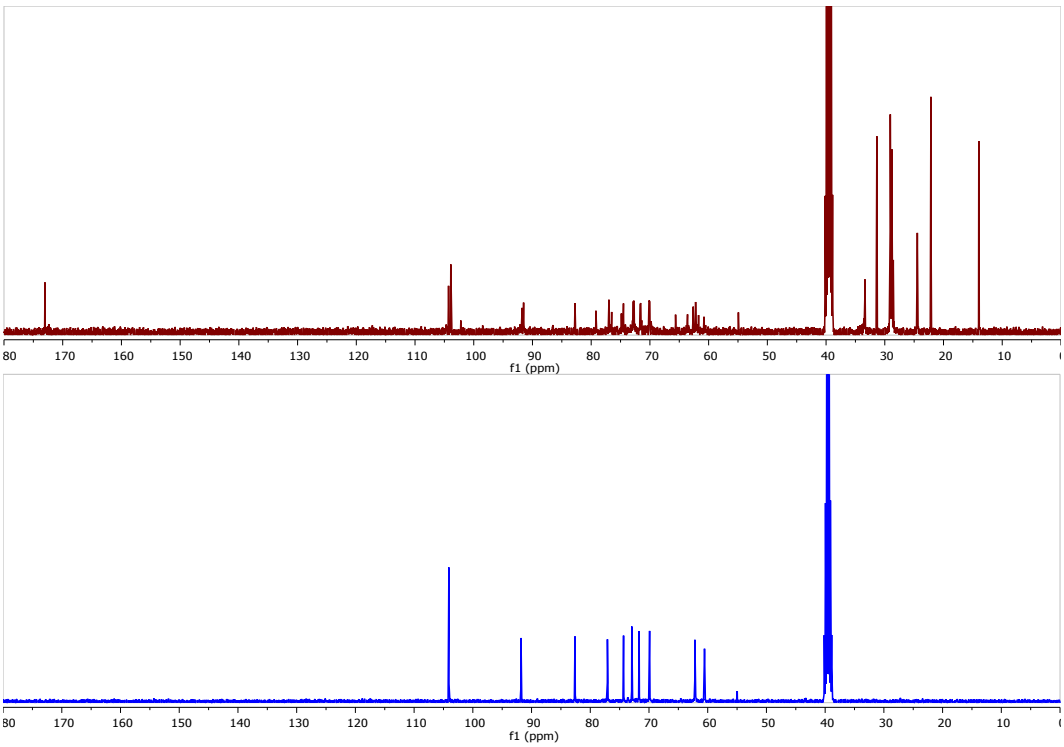

Figure SI2f – ^{13}C NMR spectrum of sucrose laurate in DMSO-d_6 (red) and sucrose in DMSO-d_6 (blue)

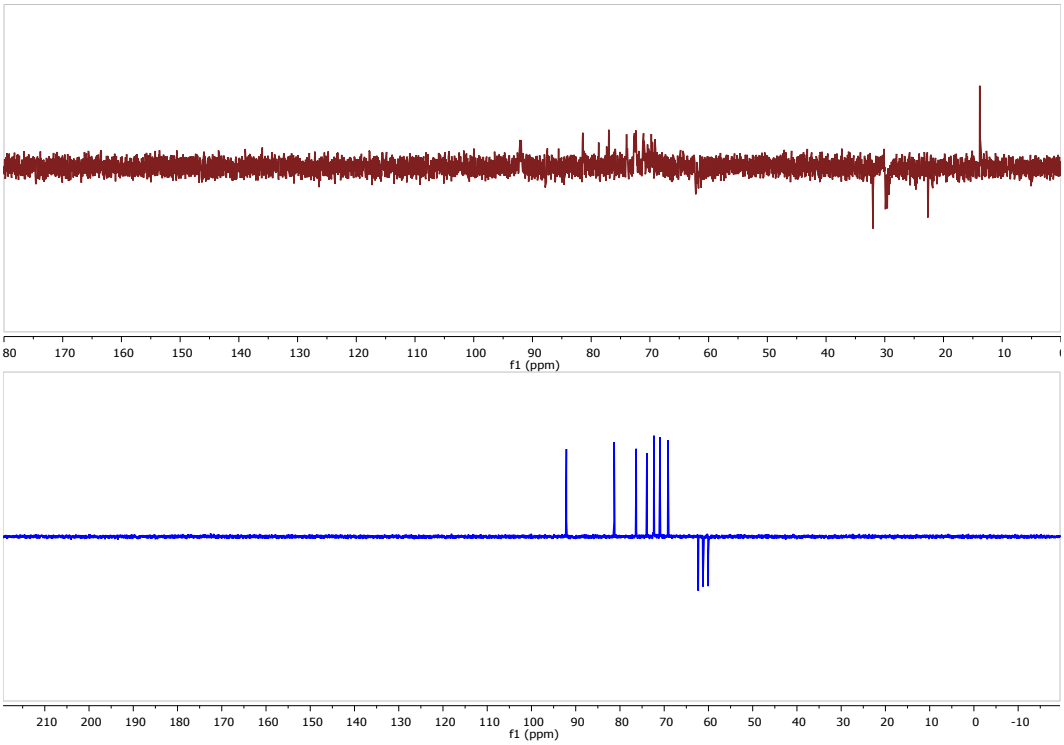

Figure SI2g – ^{13}C DEPT NMR spectrum of sucrose laurate in D_2O (red) and sucrose in D_2O (blue)

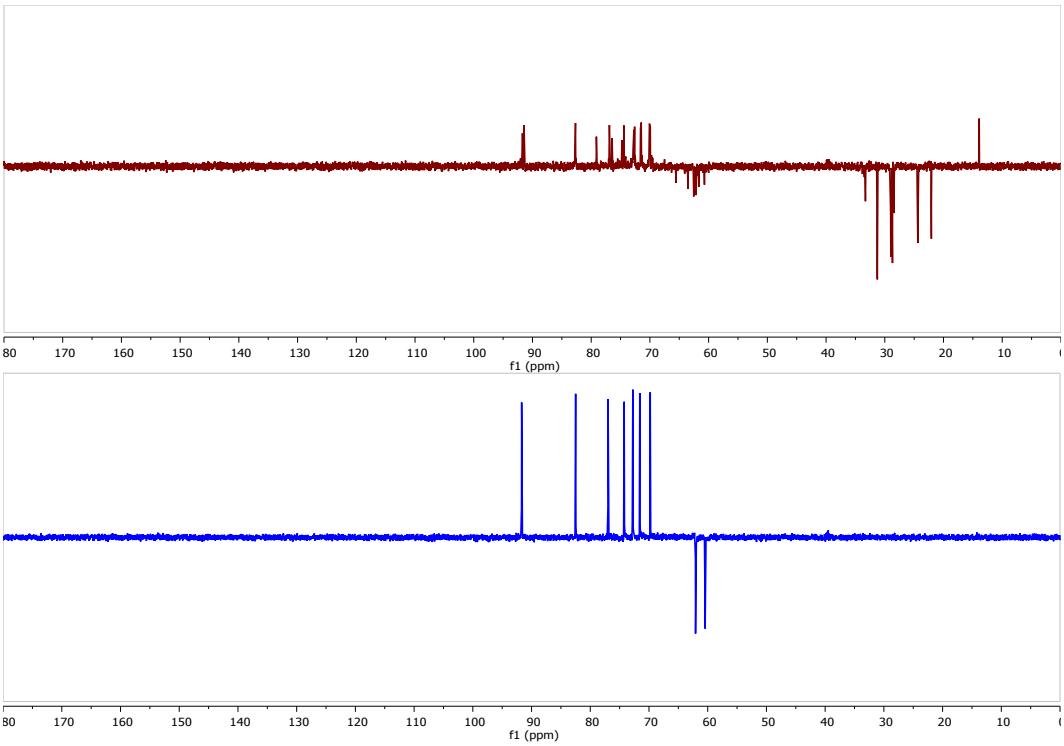

Figure SI2h – ^{13}C DEPT NMR spectrum of sucrose laurate in DMSO-d_6 (red) and sucrose in DMSO-d_6 (blue)

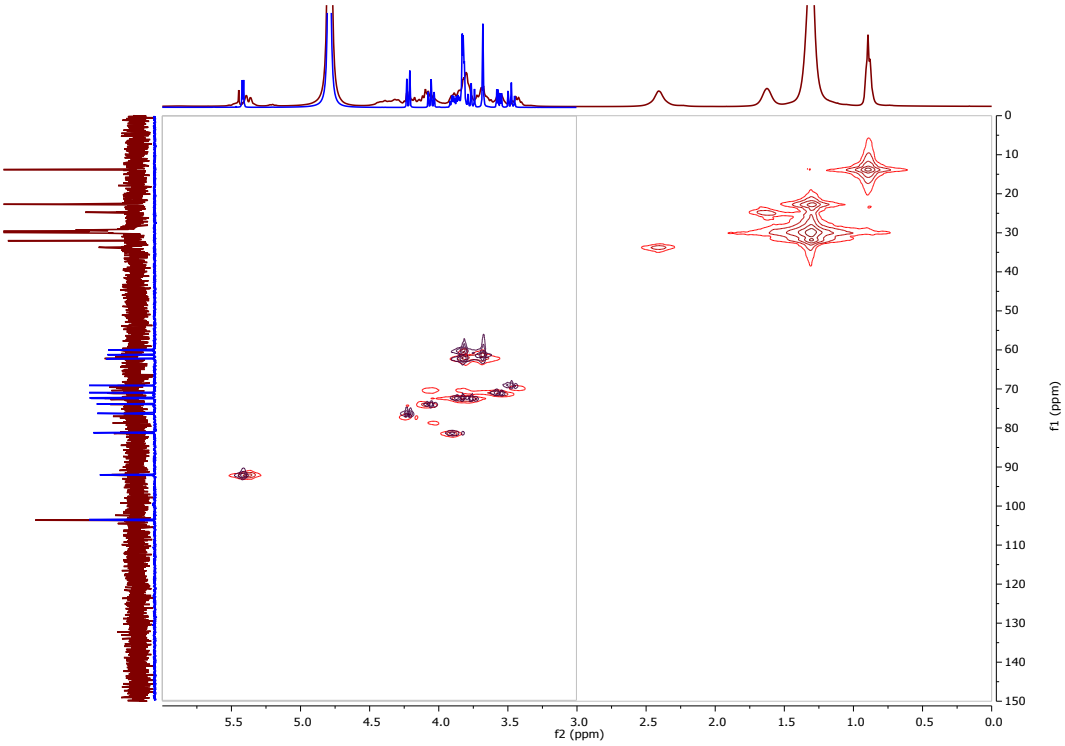

Figure SI2i– ^{1}H-^{13}C NMR (HETCOR) spectrum of sucrose laurate in D_2O (red) and sucrose in D_2O (blue)

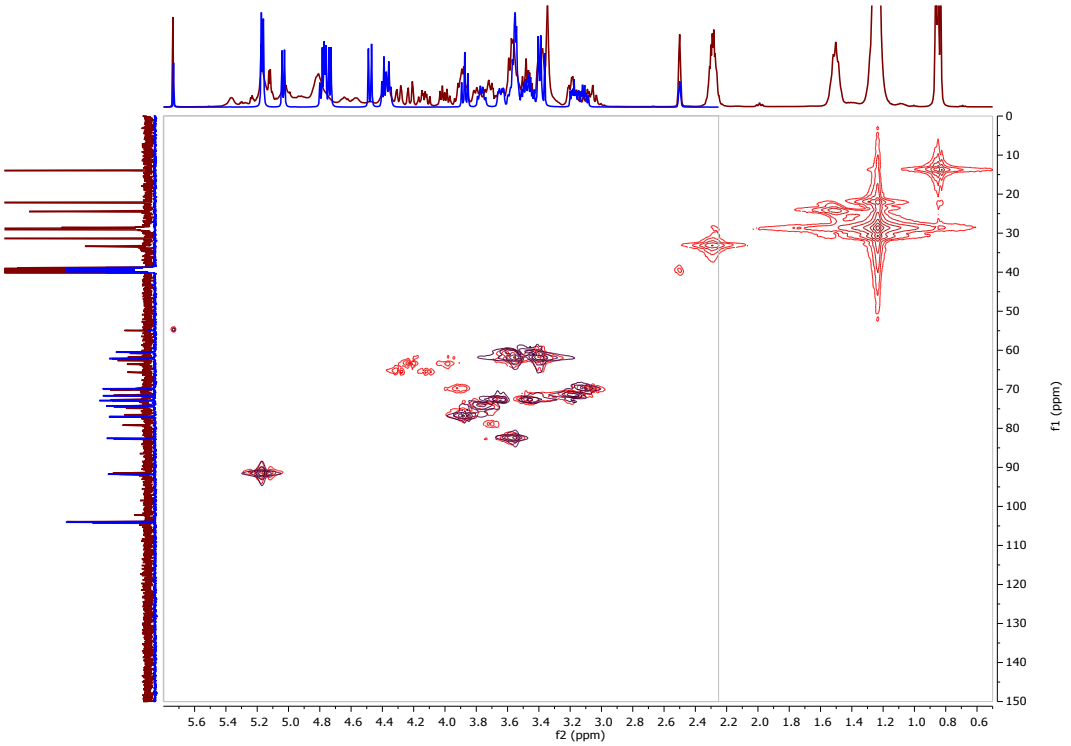

Figure SI2j– ^{1}H-^{13}C NMR (HETCOR) spectrum of sucrose laurate in DMSO-d_6 (red) and sucrose in DMSO-d_6 (blue)

High performance liquid chromatography (HPLC) – Quantification of the concentration of the di- and monosaccharide content during the digestion of a solution of sucrose laurate with invertase.

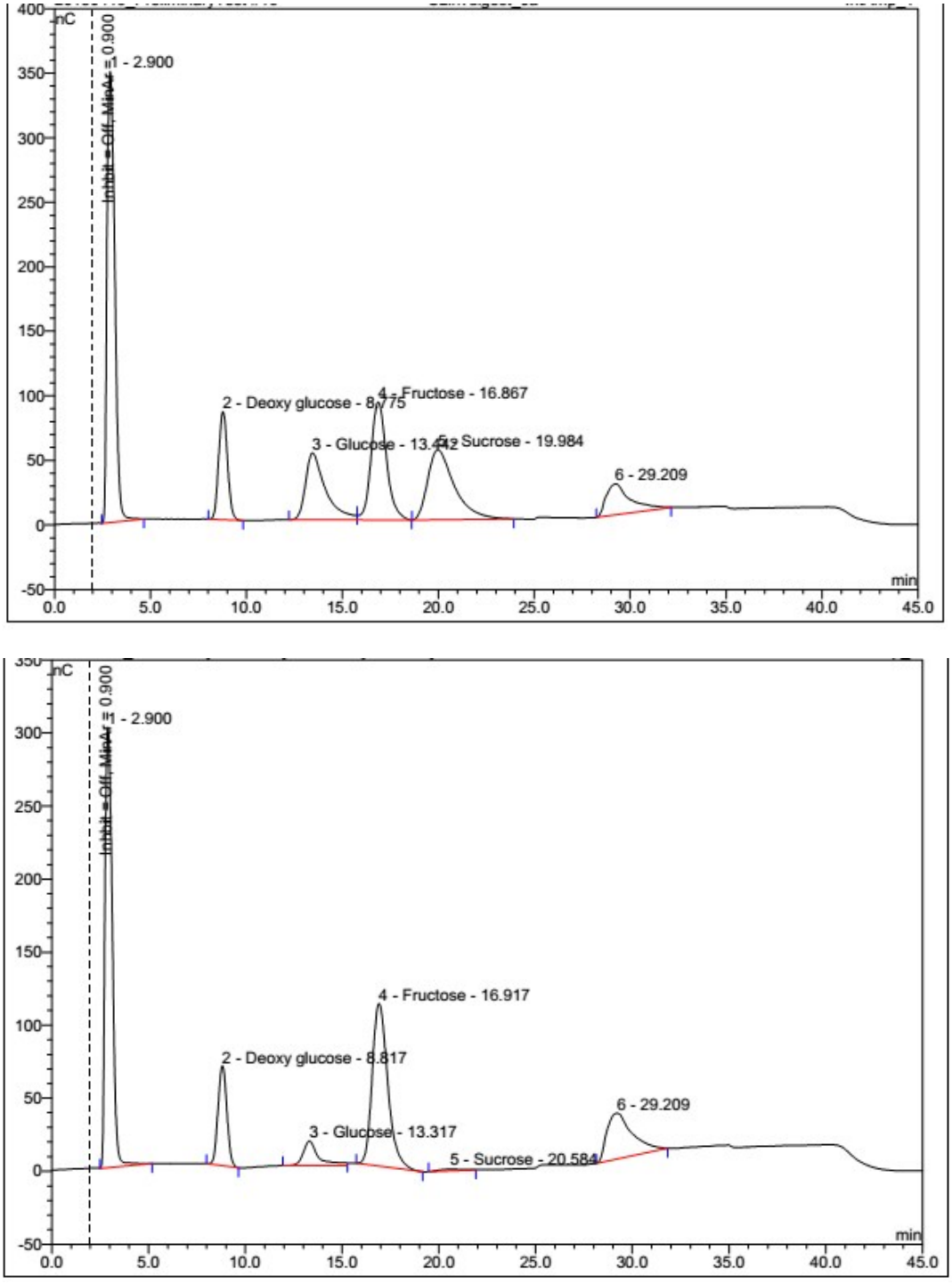

Fig. SI3 – example chromatograms of the digestion of sucrose laurate at t = 0 s (top) and 1800 s. Deoxy glucose was used as an internal standard.

Molecular Simulations – Geometrical and quantitative structure-activity relationships (QSARs) for the different amphiphilic molecules

Table SI1 – Geometrical and quantitative structure-activity relationship (QSAR) values as calculated by quantum mechanics molecular simulations in order to determine the CPP and HLB values of the amphiphiles utilised in this study.

Amphiphile	CPP	V ($Å^3$)	A_0 ($Å^2$)	L_C (Å)	HLB
Phytantriol (PHYT)	0.650	303.5	27.9	16.8	6.36
Monolinolein (MLO)	1.016	341.0	22.6	14.8	1.02
Glucose laurate (GL)	0.469	214.6	31.2	14.6	11.43
Glucose stearate (GS)	0.456	315.3	31.2	22.2	9.28
Fructose laurate (FL)	0.433	214.6	33.8	14.6	11.43
Fructose stearate (FS)	0.421	315.3	33.8	22.2	9.28
Sucrose laurate (SL-fa)	0.333	214.6	44.0	14.6	14.08
Sucrose stearate (SS-fa)	0.324	315.3	44.0	22.2	12.13
Sucrose laurate (SL-ga)	0.322	214.6	45.6	14.6	14.08
Sucrose stearate (SS-ga)	0.312	315.3	45.6	22.2	12.13

Figure SI4 – Model structures (ball and cylinders and overlapping spheres) from the molecular simulations for the different amphiphiles (first raw: xz projection; second raw : xy projection), and the corresponding geometrical and quantitative structure-activity relationship (QSAR) values as calculated by quantum mechanics molecular simulations in order to determine the CPP and HLB values of the amphiphiles utilised in this study.

A. Phytantriol (PHYT)

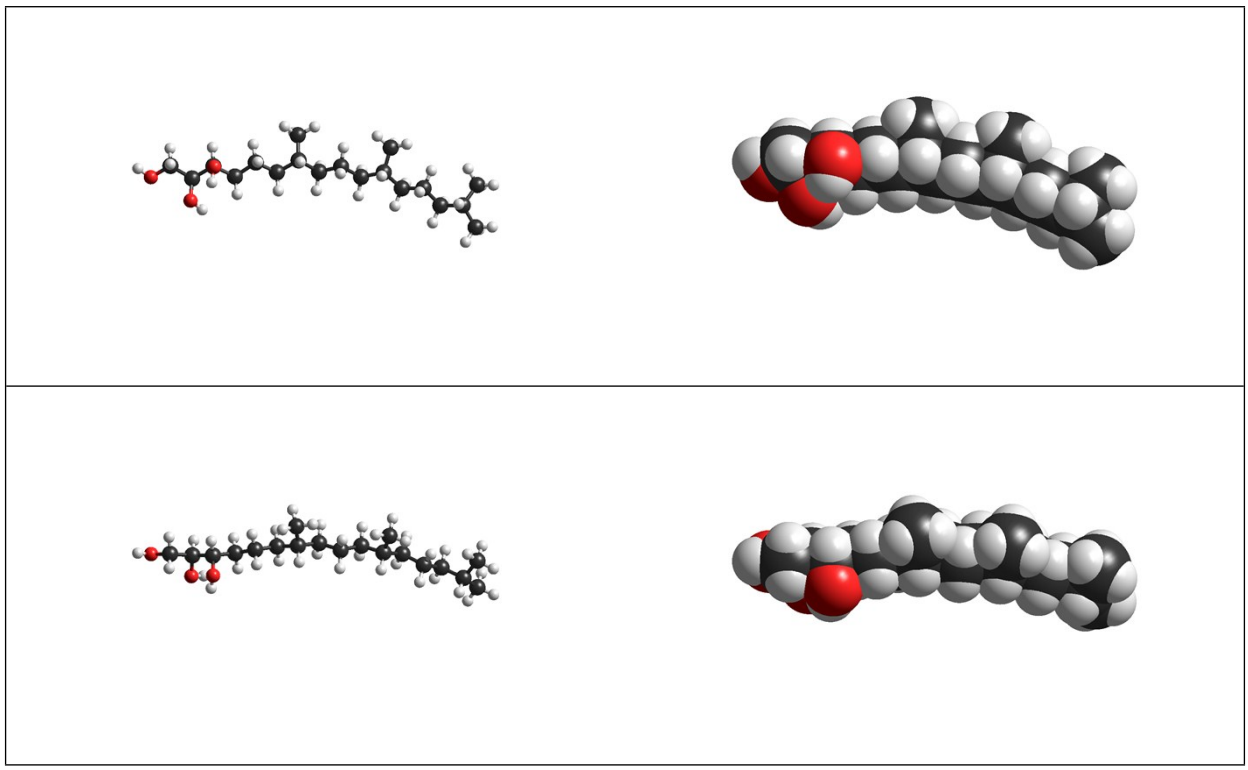

	Amphiphile	Hydrophilic	Hydrophobic
Volume (Å^3): V	350.6	82.7	303.5
Area (Å^2): A	438.5	116.5	380.1
Solvent Area (Å^2): A_S	750.0	244.8	612.5
Length (Å): L_C	21.2	4.5	16.8
Cross-sectional area (Å^2): A_0		27.9	
Hydration energy (kcal·mol^{-1})	-8.14	-16.80	0.26
log P	5.15	-1.08	5.90
HLB	6.36		
CPP	0.650		

B. Monolinolein (MLO)

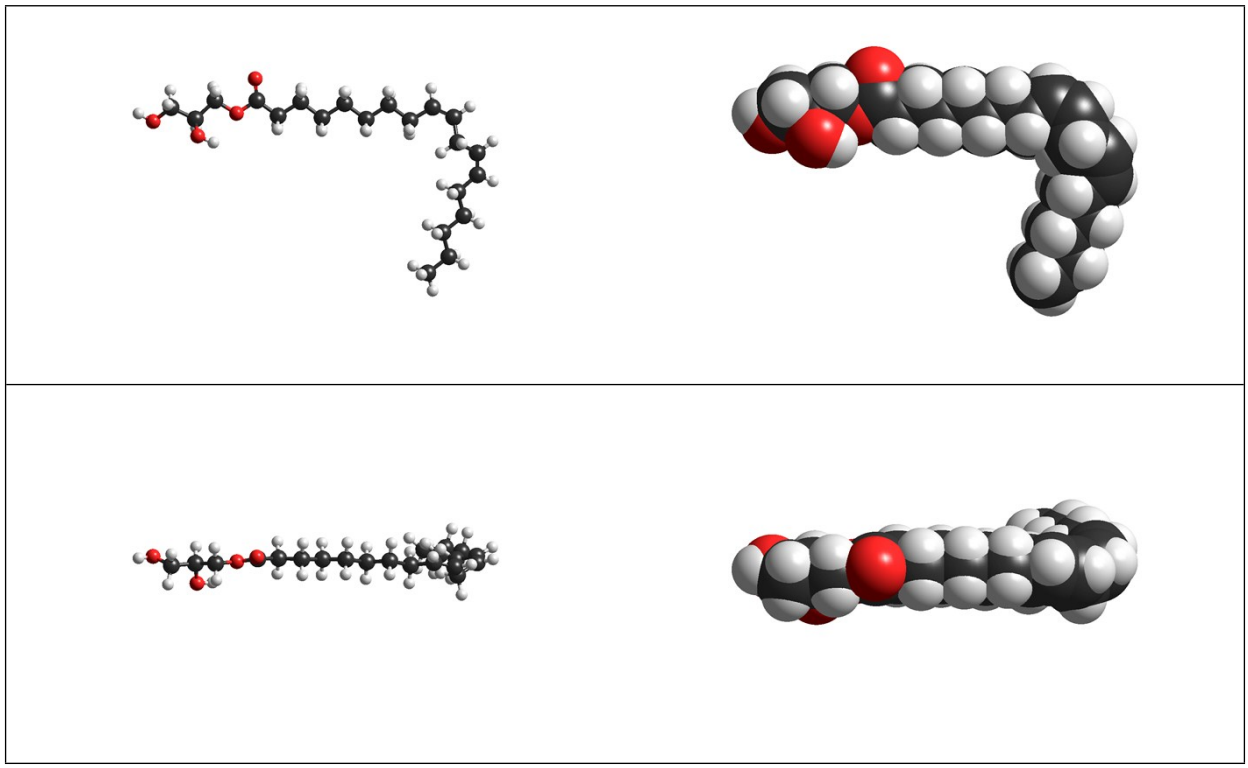

	Amphiphile	Hydrophilic	Hydrophobic
Volume ($Å^3$): V	377.0	102.0	341.0
Area ($Å^2$): A	476.8	140.6	385.2
Solvent Area ($Å^2$): A_S	791.2	288.4	650.1
Length (Å): L_C	21.6	6.8	14.8
Cross-sectional area ($Å^2$): A_0		22.6	
Hydration energy ($kcal \cdot mol^{-1}$)	-8.04	4.52	17.42
log P	5.10	-1.16	5.47
HLB	6.72		
CPP	1.016		

C. Glucose laurate (GL)

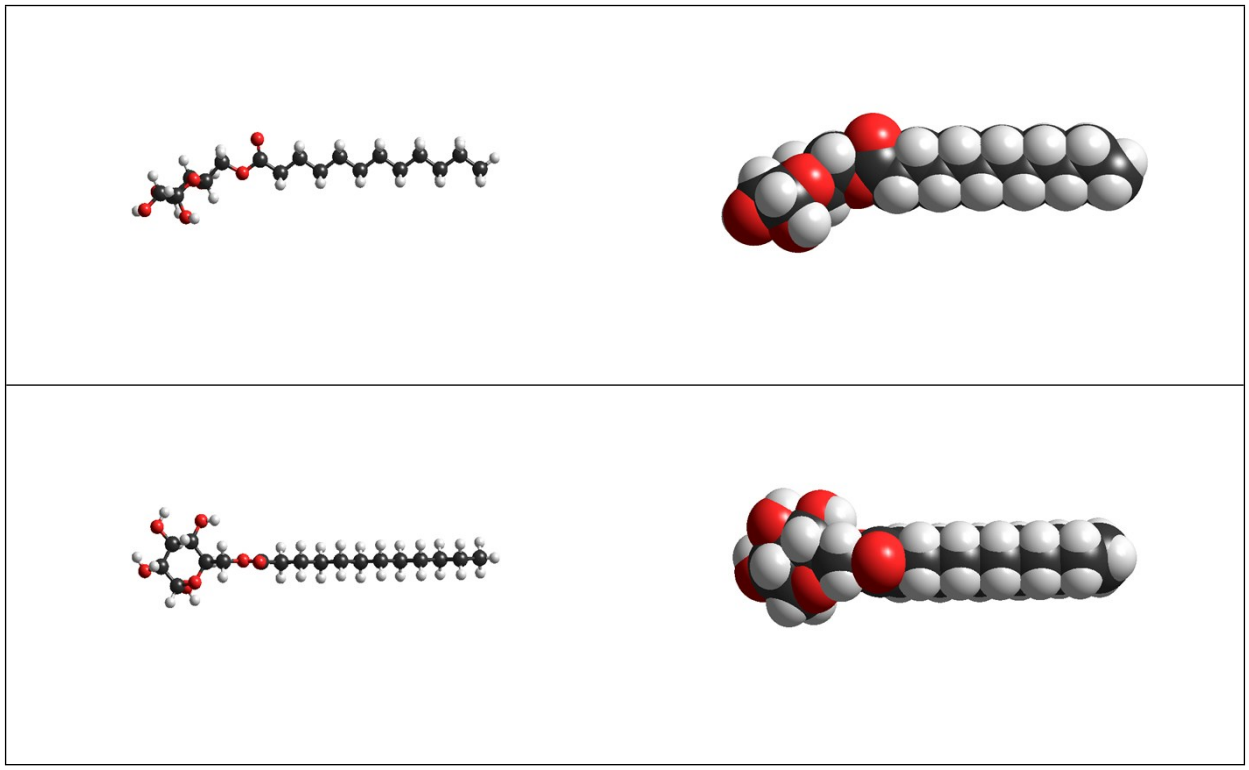

	Amphiphile	Hydrophilic	Hydrophobic
Volume (Å^3): V	347.2	162.5	214.6
Area (Å^2): A	436.4	207.7	276.5
Solvent Area (Å^2): A_S	716.1	371.5	488.1
Length (Å): L_C	22.5	7.8	14.6
Cross-sectional area (Å^2): A_0		31.2	
Hydration energy (kcal·mol^{-1})	-13.99	-2.45	17.70
log P	2.56	-1.84	3.62
HLB	11.43		
CPP	0.469		

D. Glucose stearate (GS)

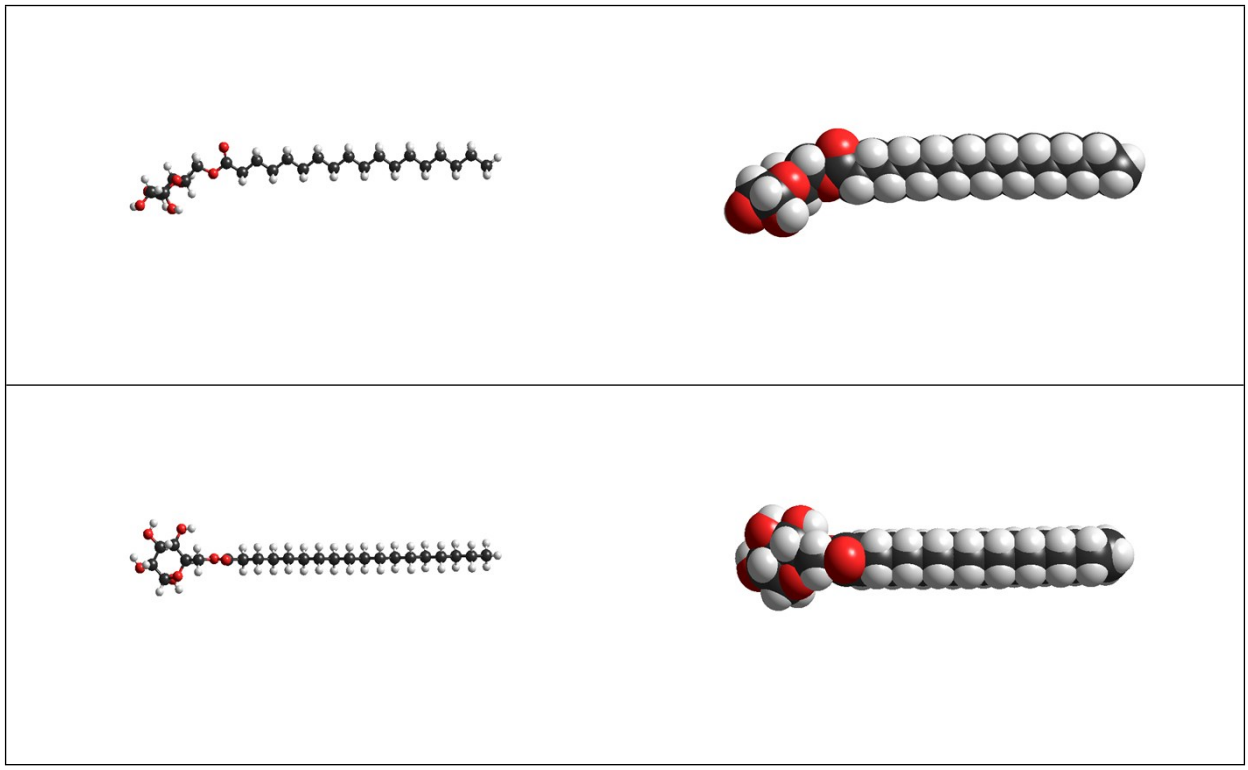

	Amphiphile	Hydrophilic	Hydrophobic
Volume (Å^3): V	447.9	162.5	315.3
Area (Å^2): A	561.5	207.7	402.7
Solvent Area (Å^2): A_S	899.9	371.5	674.1
Length (Å): L_C	30.0	7.8	22.2
Cross-sectional area (Å^2): A_0		31.2	
Hydration energy (kcal·mol^{-1})	-11.8	-2.45	19.91
log P	4.94	-1.84	5.99
HLB	9.28		
CPP	0.456		

E. Fructose laurate (FL)

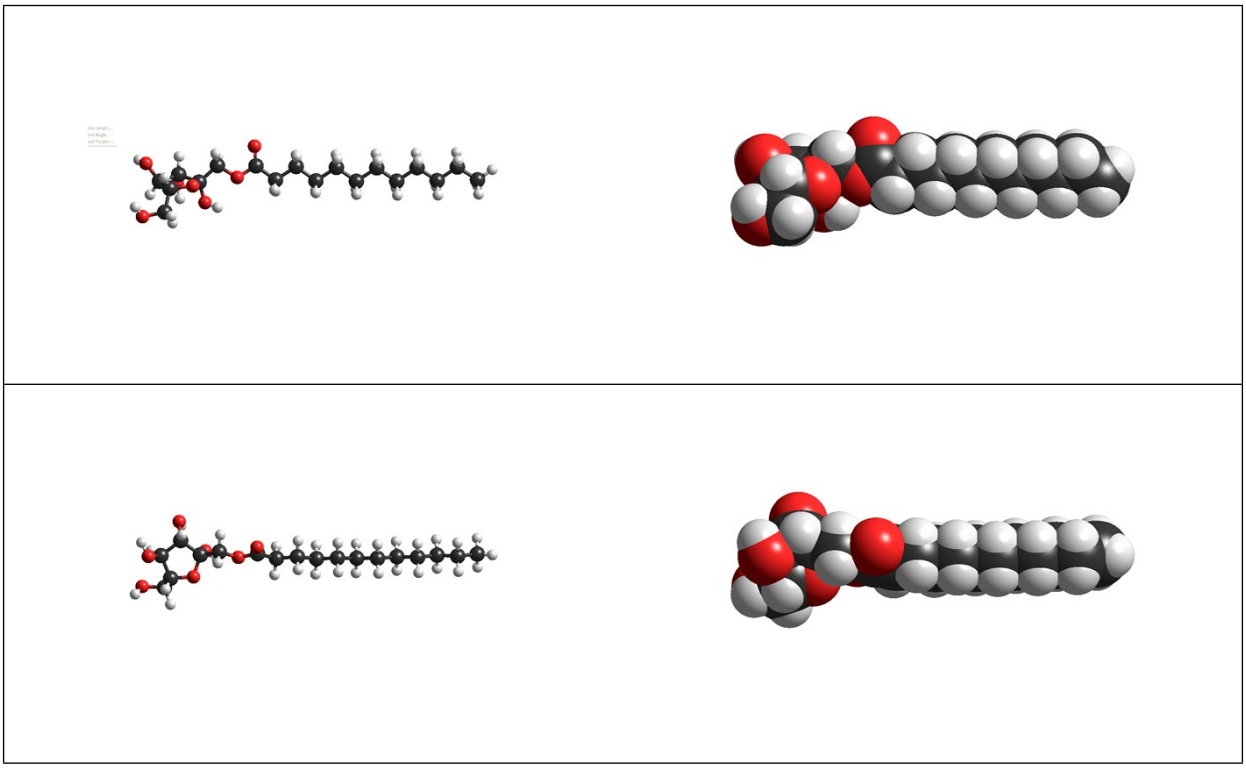

	Amphiphile	Hydrophilic	Hydrophobic
Volume (Å^3): V	348.0	163.4	214.6
Area (Å^2): A	439.7	211.3	276.5
Solvent Area (Å^2): A_S	719.4	377.8	488.1
Length (Å): L_C	21.9	7.3	14.6
Cross-sectional area (Å^2): A_0		33.8	
Hydration energy (kcal·mol^{-1})	-13.92	-2.75	17.70
log P	3.07	-1.33	3.62
HLB	11.43		
CPP	0.433		

F. Fructose stearate (FS)

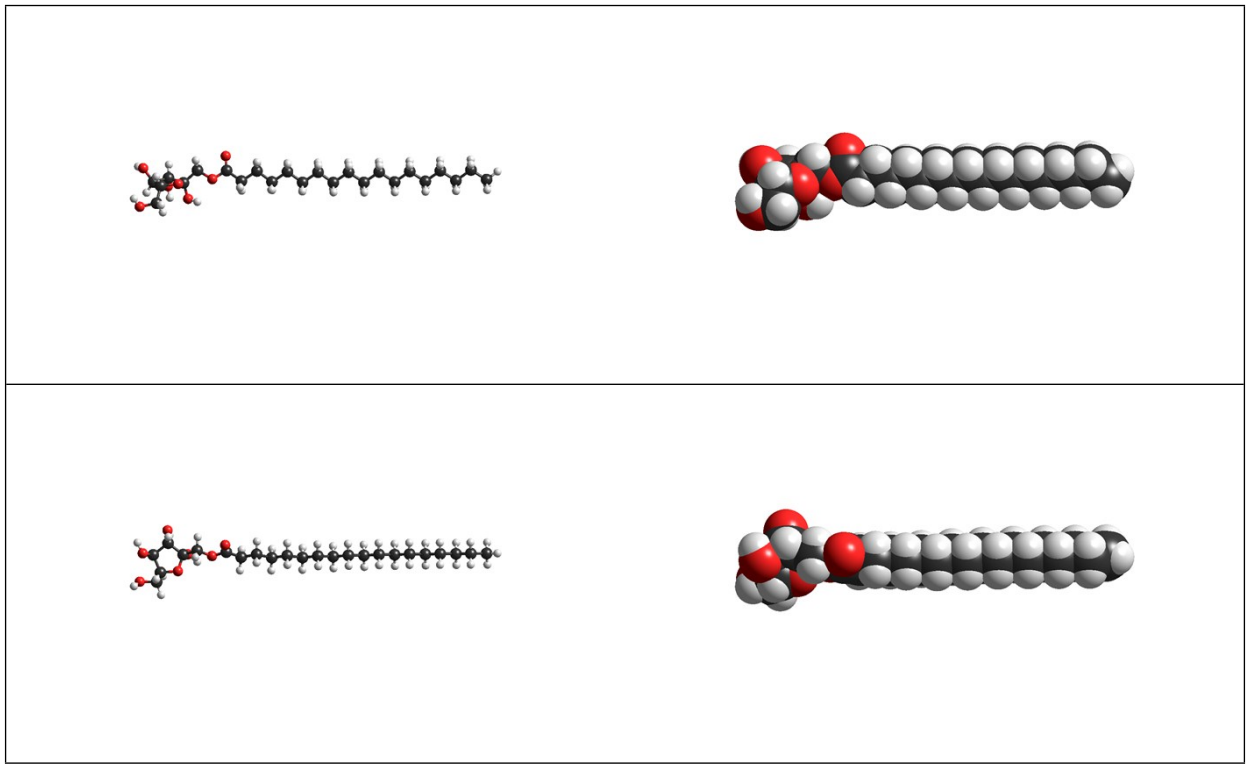

	Amphiphile	Hydrophilic	Hydrophobic
Volume (Å^3): V	448.7	163.4	315.3
Area (Å^2): A	563.8	211.3	402.7
Solvent Area (Å^2): A_S	903.5	377.8	674.1
Length (Å): L_C	29.4	7.3	22.2
Cross-sectional area (Å^2): A_0		33.8	
Hydration energy (kcal·mol^{-1})	-11.74	-2.75	19.91
log P	5.45	-1.33	5.99
HLB	9.28		
CPP	0.421		

G. Sucrose laurate (fructose-attached) (SL-fa)

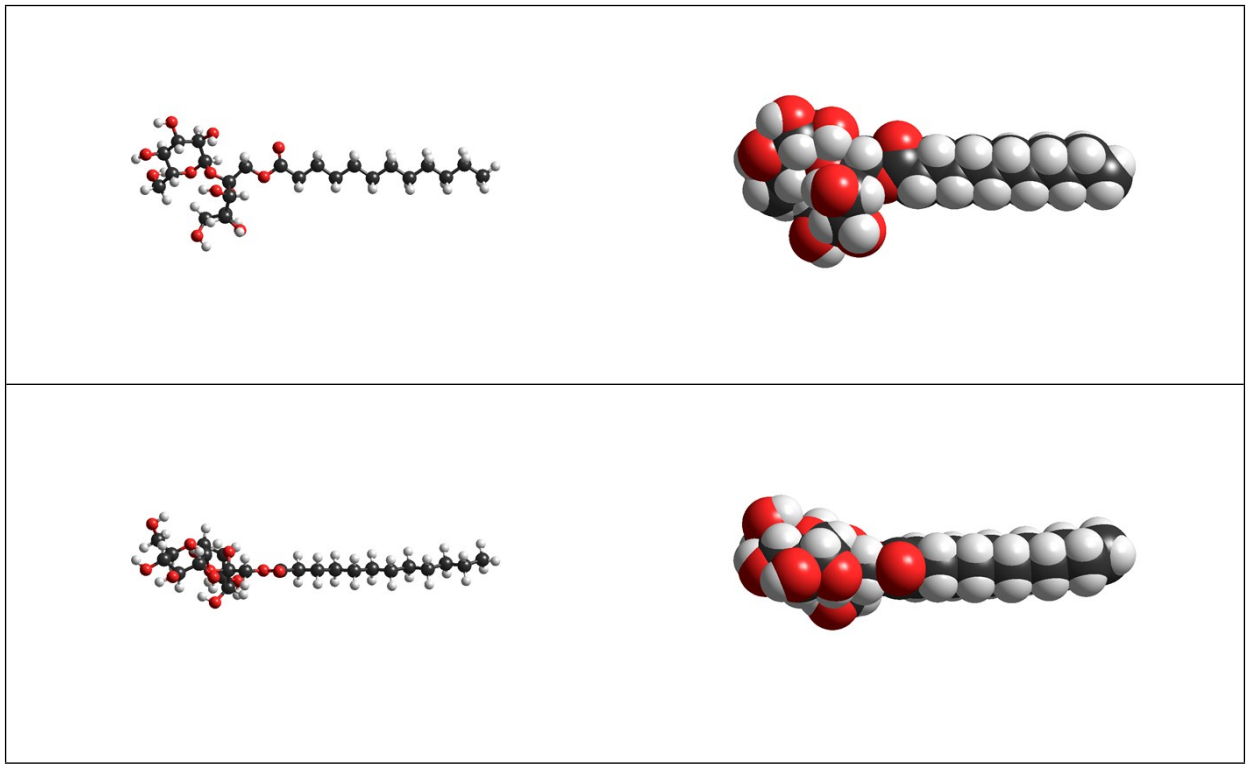

	Amphiphile	Hydrophilic	Hydrophobic
Volume (Å^3): V	474.2	289.4	214.6
Area (Å^2): A	586.4	356.7	276.5
Solvent Area (Å^2): A_S	867.5	526.3	488.1
Length (Å): L_C	24.5	9.9	14.6
Cross-sectional area (Å^2): A_0		44.0	
Hydration energy (kcal·mol^{-1})	-24.64	-15.12	17.70
log P	1.85	-2.54	3.62
HLB	14.08		
CPP	0.333		

H. Sucrose stearate (fructose-attached) (SS-fa)

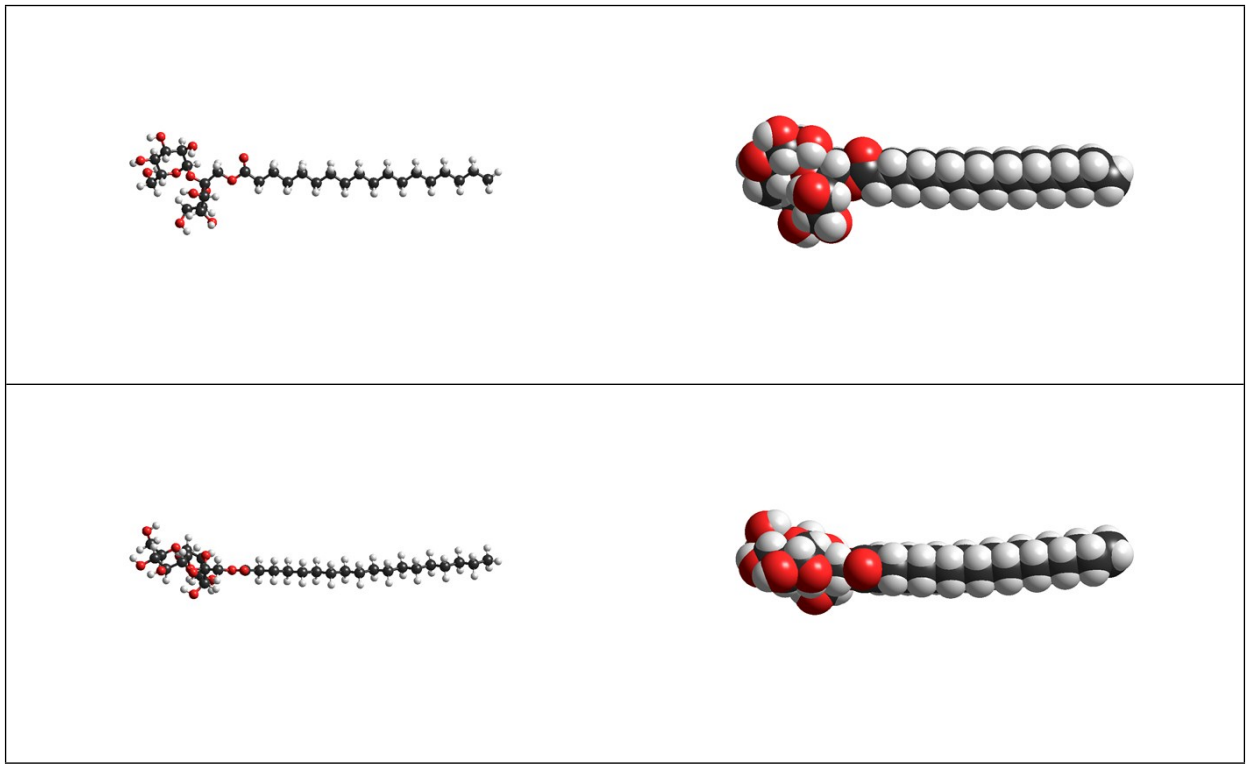

	Amphiphile	Hydrophilic	Hydrophobic
Volume (Å^3): V	574.9	289.4	315.3
Area (Å^2): A	711.3	356.7	402.7
Solvent Area (Å^2): A_S	1051.5	526.3	674.1
Length (Å): L_C	32.0	9.9	22.2
Cross-sectional area (Å^2): A_0		44.0	
Hydration energy (kcal·mol^{-1})	-22.51	-15.12	19.91
log P	4.23	-2.54	5.99
HLB	12.13		
CPP	0.324		

I. Sucrose laurate (glucose-attached) (SL-ga)

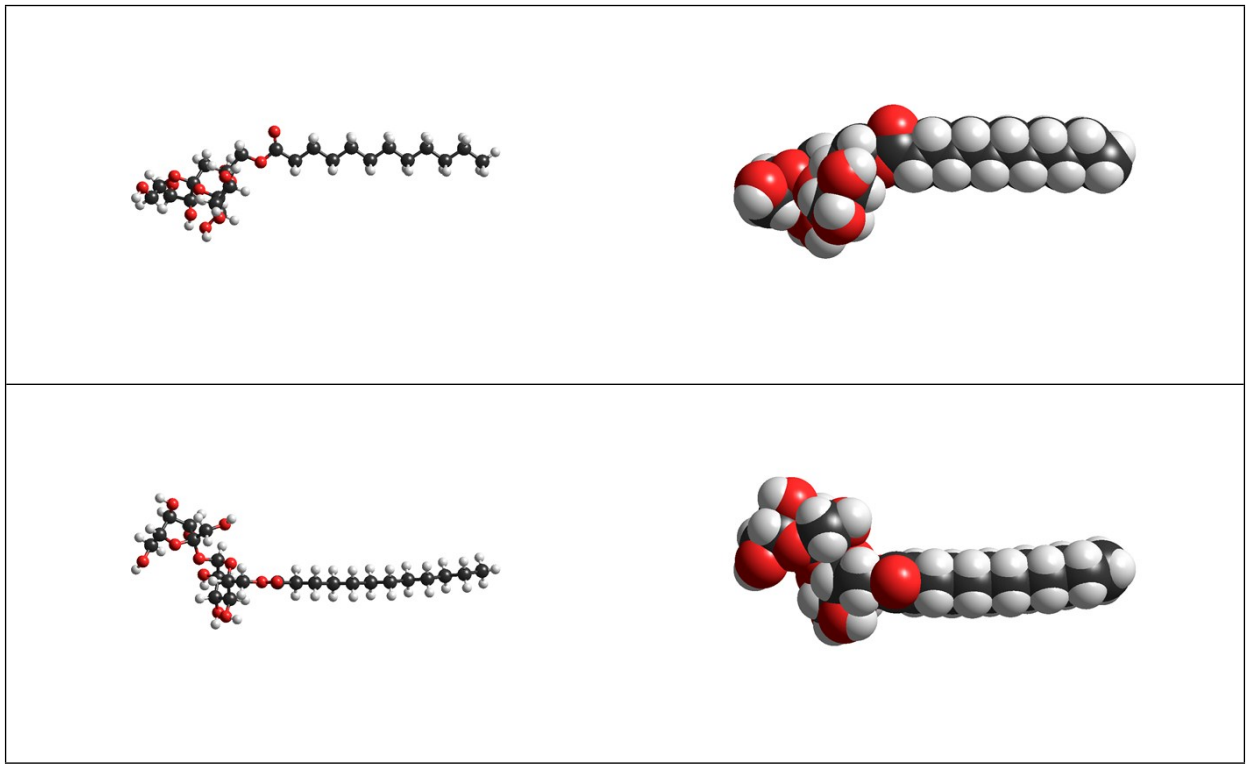

	Amphiphile	Hydrophilic	Hydrophobic
Volume (Å^3): V	467.4	289.4	214.6
Area (Å^2): A	579.4	356.7	276.5
Solvent Area (Å^2): A_S	880.8	526.3	488.1
Length (Å): L_C	24.2	9.5	14.6
Cross-sectional area (Å^2): A_0		45.6	
Hydration energy (kcal·mol^{-1})	-16.6	-15.12	17.70
log P	1.85	-2.54	3.62
HLB	14.08		
CPP	0.322		

J. Sucrose stearate (glucose-attached) (SS-ga)

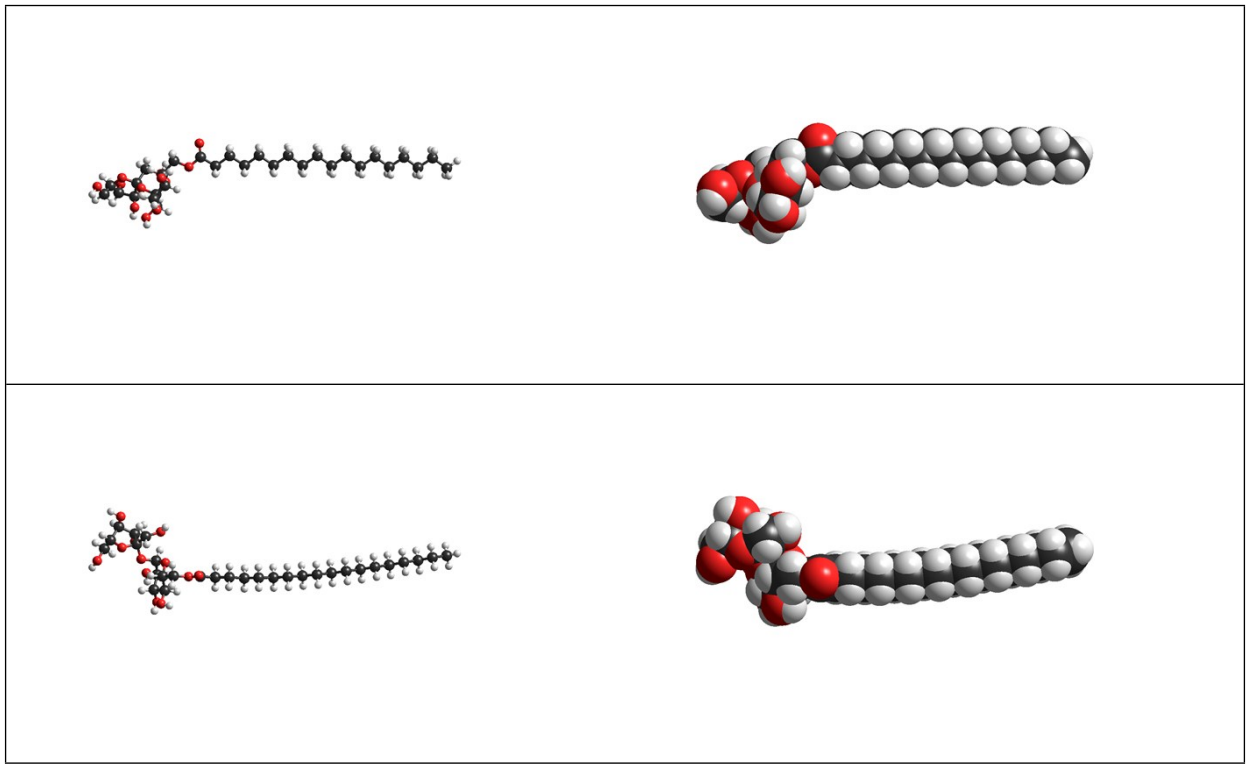

	Amphiphile	Hydrophilic	Hydrophobic
Volume (Å^3): V	569.1	289.4	315.3
Area (Å^2): A	705.5	356.7	402.7
Solvent Area (Å^2): A_S	1068.7	526.3	674.1
Length (Å): L_C	31.7	9.5	22.2
Cross-sectional area (Å^2): A_0		45.6	
Hydration energy (kcal·mol^{-1})	-14.37	-15.12	19.91
log P	4.23	-2.54	5.99
HLB	12.13		
CPP	0.312		